Functional and Structural Analysis of *cis*-Proline Mutants of *Escherichia coli* Aspartate Aminotransferase[†,‡]

Leila Birolo,[§] Vladimir N. Malashkevich,[‖,⊥] Guido Capitani,[‖] Fabio De Luca,[§] Alma Moretta,[§] Johan N. Jansonius,[‖] and Gennaro Marino*,[§]

Dipartimento di Chimica Organica e Biologica, Università "Federico II", I-80134 Napoli, Italy, and Department of Structural Biology, Biozentrum, University of Basel, CH-4056 Basel, Switzerland

ABSTRACT: To elucidate the role of the two conserved *cis*-proline residues of aspartate aminotransferase (AspAT), one double and two single mutants of the enzyme from *Escherichia coli* (*Ec*AspAT) were prepared: P138A, P195A and P138A/P195A in which the two prolines were replaced by alanine. The crystal structures of P195A and P138A/P195A have been determined at 2.3–2.1 Å resolution. The wild-type geometry, including the cis conformation of the 194–195 peptide bond is retained upon substitution of proline 195 by alanine, whereas the trans conformation is adopted at the 137–138 peptide bond. Quite surprisingly, the replacement of each of the two prolines by alanine does not significantly affect either the activity or the stability of the protein. All the three mutants follow the same pathway as the wild type for unfolding equilibrium induced by guanidine hydrochloride [Herold, M., and Kirschner, K. (1990) *Biochemistry 29*, 1907–1913]. The kinetics of renaturation of P195A, where the alanine retains the wild-type cis conformation, is faster than wild type, whereas renaturation of P138A, which adopts the trans conformation, is slower. We conclude that *cis*-prolines seem to have been retained throughout the evolution of aspartate aminotransferase to possibly play a subtle role in directing the traffic of intermediates toward the unique structure of the native state, rather than to respond to the needs for a specific catalytic or functional role.

Proline residues have been recognized to be of special significance for protein architecture (for reviews see refs *1* and *2*). Proline, actually, is unique among natural amino acids in proteins since its cyclic nature prevents rotation about the N–C$_\alpha$ bond and the peptide backbone has no amide hydrogen for use as a donor in hydrogen bonding. Moreover, because of the very small difference in steric hindrance between cis and trans conformations, the trans form is only slightly favored. A statistical evaluation of the protein structures deposited in the Brookhaven Protein Data Bank revealed that proline is the fourth most conserved residue type in terms of substitution with other amino acids and *cis*-proline even the second most conserved residue type, after the most conserved half-cystine (*3*), thus suggesting a specific structural role for *cis*-proline. Proline is considered to favor protein stability because its cyclic nature restricts the conformations available to the unfolded state (*4*). Exchanging a *cis*-proline for any other amino acid usually has a greater

unfavorable effect on protein stability than just increasing the conformational entropy of the unfolded state. Upon substitution, indeed, the protein can either retain the cis conformation in the newly generated peptide bond or adopt the trans conformation. Both choices are thermodynamically costly: the former because the free energy difference between the cis and trans isomer is much higher for all of the other residues than for a proline, the latter because the polypeptide chain around the mutated residue must accommodate the backbone isomerization.

The cis/trans isomerization is rate-limiting in the folding of a number of proteins, such as thioredoxin (*5*), RNase A (*6*), and RNase T1 (*7*). Substitutions of cis imide bonds with trans amide ones in the above single-domain monomeric proteins simplify the folding processes by eliminating slow-folding species.

In this paper we report the characterization of three mutant forms of *Escherichia coli* aspartate aminotransferase (*Ec*AspAT)[1] in which the two highly conserved *cis*-prolines were replaced by alanine.

[1] Abbreviations: *Ec*AspAT, aspartate aminotransferase from *Escherichia coli*; WT, wild-type *Ec*AspAT; P138A and P195A, single proline-to-alanine mutants of *Ec*AspAT; P138A/P195A, double proline-to-alanine mutant of *Ec*AspAT; cAspATp, porcine cytosolic aspartate aminotransferase; N$_2$, M, M*, and U, native dimer, two distinct folding intermediates, and the unfolded state of *Ec*AspAT, respectively; CD, circular dichroism; GuHCl, guanidine hydrochloride; DTT, dithiothreitol; EDTA, disodium ethylenediaminetetraacetic acid; HEPES, *N*-(2-hydroxyethyl)piperazine-*N*′-2-ethanesulfonic acid; PEG, poly(ethylene glycol); PLP, pyridoxal 5′-phosphate; PMP, pyridoxamine 5′-phosphate; NADH, reduced β-nicotinamide adenine dinucleotide.

The evolution of aminotransferases has been studied in detail by Christen and colleagues, who identified four evolutionarily related protein subgroups (*8*). Conclusive information on the structural or functional role of the 11 invariant residues of subgroup I of aminotransferases, with the exception of the pyridoxal 5′-phosphate-binding lysine, is as yet solely available for aspartate aminotransferase, the best characterized of the members of subgroup I (*9*). Among these very few invariant residues, most of which are involved in the binding of the coenzyme in the active site (*10*), there are two prolines that are in cis conformation in all of the AspATs for which the three-dimensional structure is known. AspATs are invariably homodimers with two identical and independent active sites located at the subunit interface. Each subunit can be divided into an N-terminal arm (in the case of *E. coli* enzyme, spanning from Met5 to Asp15), a large cofactor-binding domain (Lys46 to Arg329), and a small domain (Pro16 to Lys45 and Ile 330 to Leu 409) (*11*), the residue numbering being based on the sequence alignment to the first and longest AspAT sequence, that of porcine cytosolic AspAT (cAspATp) (*12*). Each active site consists of residues from the large domains of both subunits and one of the small domains, and a key feature of the catalytic mechanism of this enzyme is the rearrangement of the domain structure upon substrate binding, with a net rotation of the small domain with respect to the large domain. Both *cis*-prolines, Pro138 and Pro195, are in loop regions of the large domain close to the interface between the small and the large domains (*13*). Although neither of them makes direct contact to any residue of the small domain in wild-type *Ec*AspAT, because of their distinctive location in the structure of this enzyme, an involvement of Pro138 and/or Pro195 in the functional flexibility of the protein is possible, too. Moreover, the mutation of *cis*-proline residues in a large oligomeric protein can be usefully compared with analogous studies performed thus far on much smaller and simpler proteins.

To better understand the role of these invariant residues, three mutants of *Ec*AspAT have been constructed (P138A, P195A, and P138A/P195A). Herein, the three-dimensional structures of two of them at 2.3−2.1 Å resolution are reported together with a kinetic and a thermodynamic characterization of the mutants.

MATERIALS AND METHODS

Materials and Buffers. *E. coli* cell TY103 (*14*) and plasmid pKDHE19 (*15*) were kind gifts from Prof. P. Christen, Biochemiches Institut der Universität Zürich, Switzerland. Sodium cyanoborohydride, malate dehydrogenase, aspartic acid, and L-cysteinesulfinic acid were purchased from Sigma; ultrapure guanidine hydrochloride was from Calbiochem. Synthetic oligonucleotides were from Primm and Genenco. All other reagents were of analytical grade.

Oligonucleotide-Directed Mutagenesis. Site-directed mutagenesis of the *aspC* gene was performed by the polymerase chain reaction on the *aspC* gene [inserted in the expression plasmid pKDHE19 (*15*)]. The mutagenic primers were P138A (5′-CGGCCAG<u>GCT</u>AGCGTTGCTCAC-3′), its complementary P138AR (the mutated nucleotides are underlined), P195A (5′-CAGCGTAGG**A**TCGATACCGGTTGCGTTAT-GGCAG-3′), and its complementary P195AR (boldface type

was used to indicate the mutation to introduce a *Cla*I site). Two other external oligonucleotides were needed to amplify the whole region from nucleotides 10 to 870 of the gene: P1 (5′-GAACATTACCGCCGCTCCTG-3′) and P298A (5′-CCGTGTGCTGGTGCGTTAGAGTAGTTAGCGCG-3′).

Three separate PCRs were carried out on the *aspC* gene [inserted in the expression plasmid pKDHE19 (*15*)]: from nucleotides 10 to 494 (P1 and P138AR), 473 to 674 (P138A and P195AR), and 645 to 870 (P195AR and P298A), respectively. The amplifications were carried out in 50 μL with 2.5 units of Vent$_R$ polymerase (New England Biolabs) using 10 ng of supercoiled pkDHE19, 1 pmol/μL primer, and 200 μM dNTP. Annealing was for 1 min at 55 °C, and polymerization was for 1 min at 74 °C for 20 cycles. Amplified fragments were purified by agarose gel electrophoresis, and after denaturing and annealing the three fragments, another PCR was carried out with the external primers (P1 and P298A) to recover the whole fragment from nucleotides 10 to 870.

The PCR product was ligated into *Bcl*I- and *Nsi*I-digested pKDHE19 to generate the plasmid P138A/P195A, containing both the P138A and the P195A mutations.

The entire sequence of the *Bcl*I−*Nsi*I insert of P138A/P195A was determined using a T7 Sequencing Kit (Pharmacia Biotech).

To obtain the two single mutant genes, the 266 bp *Bcl*I−*Nco*I fragments (containing position 138) were exchanged between pKDHE19 and P138A/P195A, thus generating the P138A and P195A plasmids. Single colonies of transformants were picked and screened for the presence of the desired mutations by restriction analysis, since *Nhe*I and *Cla*I endonuclease sites had been introduced in the mutagenizing oligonucleotides.

Protein Expression and Purification. Wild-type and mutant *Ec*AspATs were isolated from the overproducing *E. coli* strain TY103 (*14*) harboring either the plasmid pKDHE19 or the same plasmid carrying the mutated genes for the P138A, P195A, and P138A/P195A AspATs. Bacteria were grown and protein purified as described previously (*16*). The enzyme preparations were homogeneous to SDS−PAGE. The purified enzymes were stored at −80 °C in the presence of 1 mM DTT and an excess of PMP and 2-oxoglutarate.

Subunit concentrations of *Ec*AspAT were determined spectrophotometrically on a Beckmann DU7500 spectrophotometer, using $\epsilon_{280} = 49935$ M^{-1} cm^{-1} (*17*).

All experiments were carried out on the PLP form of the enzymes, obtained by removal of excess PMP and 2-oxoglutarate either by extensive dialysis against appropriate buffer or by gel filtration on a Superose 12 PC column (3.2 × 30 mm) using the SMART system (Pharmacia).

Crystallization and X-ray Diffraction Data Collection. Crystals of the P195A and P195A/P138A mutants were grown using the hanging drop vapor diffusion method. Drops of 4 μL containing 20 mg/mL protein, 10 mM K-phosphate, 10 μM PLP, 2 mM K$_2$-EDTA, and 0.5 mM DTT were mixed with an equal volume of reservoir solution containing 1.9−2.1 M ammonium sulfate, 0.2 M 2-methylmorpholine, and 2% PEG 400 and equilibrated against 1 mL of this reservoir solution. Maleate (20 mM) was added to the protein solution to obtain the maleate complex of the P195A/P138A mutant. Usually crystals appeared in 3−4 weeks and reached a maximum size of 0.3 × 0.3 × 2.0 mm^3. However, only a

few crystals could be used for data collection because of twinning. Diffraction data using Cu Kα radiation were collected on a MarResearch imaging plate. These crystals belong either to the space group $C222_1$ (*18, 19*) or to the space group $P2_1$ with pseudo $C222_1$ symmetry (*11*). To resolve this ambiguity for the mutant crystals, we processed the diffraction data from the same crystal of the unliganded P195A mutant in both the orthorhombic and the monoclinic systems and refined the resulting structures independently (Table 1). The diffraction data for the maleate complex of the P195A/P138A mutant unfortunately could be processed only in space group $C222_1$, since the only available crystal dissolved during data collection, and the monoclinic data would have been only 60% complete. Intensities were integrated with the program XDS (*20*), scaled with AGRO-VATA and ROTAVATA, and truncated to structure factors with TRUNCATE (all from the CCP4 program suite, 1992).

Structure Solution and Refinement. The structures were solved by the molecular replacement method using the program AmoRe (*21*) and high-resolution wild-type *Ec*AspAT structures as a trial model (*19*). Model building and electron density interpretation were done with O (*22*). The structures were refined (Table 1) using TNT (*23*). Secondary structure analysis was done with the program PROMOTIF (*24*).

Enzymatic Activity Assays. During purification, enzymatic activity was routinely measured by the conventional malate dehydrogenase-based assay (*25*), the conditions being 25 °C in 0.1 M Na-HEPES buffer solution, pH 8.0, 18 mM aspartate, 7 mM 2-oxoglutarate, and 0.15 mM NADH, containing malate dehydrogenase (2.5 μg/mL).

Determination of Transamination Kinetic Parameters. Kinetic parameters for the substrate pair aspartate/2-oxoglutarate were calculated at 25 °C in 50 mM Na-HEPES, pH 7.5, from the initial steady-state rates determined in the malate dehydrogenase-coupled assays in a matrix of four concentrations of aspartate at each of four concentrations of 2-oxoglutarate. The data were fitted by nonlinear regression to the equation (*26*):

$$\frac{v}{[E_t]} = \frac{k_{cat}[Asp][Oxo]}{K_{MAsp}[Oxo] + K_{MOxo}[Asp] + [Asp][Oxo]} \quad (1)$$

where K_{MAsp} and K_{MOxo} are the Michaelis constants for aspartate (Asp) and 2-oxoglutarate (Oxo), respectively, and k_{cat} is the catalytic constant. No substrate-dependent inhibition was noted at the highest concentrations employed.

Determination of Maleate Dissociation Constant by Direct Titration. A 10 μM enzyme solution in 50 mM HEPES, pH 7.5, was titrated by directly adding small aliquots of concentrated ligand solution, and the increase in absorbance at 436 nm was measured. Dissociation constants were obtained from absorbance data as already reported (*27*).

Spectrophotometric Determination of pK_a Values. The pK_a of the internal aldimine double bond between lysine 258 and PLP was determined from the absorbance at 430 nm of spectra of AspATs recorded at different pH values and by fitting the experimental data with the equation (*28*):

$$A = \frac{A_1 - A_2}{1 + 10^{pH - pK_a}} + A_2 \quad (2)$$

Table 1: Data Collection and Refinement Statistics

	P195A		P138A/ P195A	P138A/ P195A + maleate
space group	$P2_1$	$C222_1$	$P2_1$	$C222_1$
resolution (Å)	10.0−2.1	10.0−2.1	10.0−2.1	10.0−2.3
R_{sym}	0.058	0.056	0.065	0.082
no. of reflections	59668	30049	58133	21779
completeness (%)	92.2	92.0	91.3	90.0
R-factor[a]	0.197	0.186	0.207	0.206
no. of protein atoms	6164	3082	6160	3080
no. of solvent atoms	515	254	688	365
Ramachandran plot				
core region	92.5	92.2	91.1	90.8
allowed region	7.2	7.5	8.3	8.9
disallowed region	0.3	0.3	0.3	0.3
mean B-factor (Å^2)				
entire molecule	35.1	35.4	34.2	42.5
main chain	30.3	30.6	29.6	38.2
side chains	40.3	40.6	39.1	47.1
solvent	61.4	62.0	66.7	71.9
rmsd from ideality				
bond distances (Å)	0.010	0.012	0.011	0.012
bond angles (deg)	1.14	1.18	1.16	1.84
planar groups (Å)	0.008	0.009	0.008	0.006

[a] R-factor $= \sum ||F_o| - |F_c||/\sum |F_o|$.

where A_1 and A_2 are the higher and lower absorbance limits at 430 nm, respectively.

The buffers used were K-MES (4-morpholineethane-sulfonic acid) in the pH range 5.50−6.60, K-MOPS (4-morpholinepropanesulfonic acid) in the pH range 6.50−7.54, K-EPPS [4-(2-hydroxyethyl)-1-piperazinepropanesulfonic acid] in the range 7.30−8.72, and K-CHES [2-(cyclohexylamino)-ethanesulfonic acid] in the pH range 9.03−10.08. The spectra were recorded at 25 °C, at a buffer concentration of 50 mM and 0.1 M KCl, and the enzyme concentration was 9 μM. All solutions have been filtered before use.

The pK_a determinations in the presence of maleate were conducted as above but in the presence of 50 mM maleate.

Kinetics of Reduction with Sodium Cyanoborohydride. The enzymes, 8 μM, in 50 mM HEPES, pH 7.5, were treated at 25 °C with 10 mM NaBH$_3$CN in the presence of different fixed concentrations of maleate. The increase in absorbance at 330 nm, due to the reduction of the aldimine double bond between lysine 258 and PLP in the active site of the enzyme, was followed with time, and the pseudo-first-order kinetic constant was calculated. Further analysis of the data resulting from the reduction experiments was accomplished using the equilibrium scheme and eq 3 reported in ref *29*:

$$k_{obs} = \frac{k'(K_a + [M])}{r[M] + K_a} \quad (3)$$

Thermal Unfolding Monitored by CD Spectroscopy. Thermal denaturation of the protein was followed by recording temperature-induced changes in secondary structure. Ellipticity at 221 nm was measured as the temperature was varied from 25 to 80 °C at a rate of 1 °C min^{-1}. A Jasco J500 spectropolarimeter equipped with a thermostatically controlled cuvette was used, and temperature was measured directly in the 0.1 cm path-length quartz cell. Enzyme concentration was 3.9 μM in 10 mM HEPES, 1 mM DTT, and 0.15 M NaCl, pH 7.5.

Linear baselines were fitted above and below the transition zone, and the apparent fraction of molecules in the unfolded state (F_u) has been derived from the experimental mean residue ellipticity according to the equation:

$$F_u = \frac{(y_n - y_{obs})}{(y_n - y_u)} \qquad (4)$$

where y_n and y_u are the pre- and posttransitional baselines that are assumed to depend linearly on temperature:

$$y_n = y_n{}^0 + m_n T$$

$$y_u = y_u{}^0 + m_u T$$

The midpoint of thermal transition, T_m, was defined as the temperature at which the apparent fraction F_u is = 0.5.

GuHCl-Induced Unfolding. Native *Ec*AspAT holoenzyme (3.9 μM in10 mM HEPES, pH 7.5, 1 mM DTT, and 0.15 M NaCl) was incubated at 25 °C in the presence of various concentrations of GuHCl for 1 h (folding/unfolding equilibrium was attained within 30 min, as determined in preliminary experiments by following with time the enzymatic activity and fluorescence). The extent of unfolding was determined by analyzing hydrodynamic behavior, tryptophan fluorescence, and amide bond ellipticity.

For hydrodynamic measurements, 50 μL of the samples, 3.9 μM in 10 mM HEPES, pH 7.5, 1 mM DTT, and 0.15 M NaCl equilibrated at different concentrations of GuHCl, was loaded on a Superose 12 PC (3.2 × 300 mm) gel filtration column installed on the Smart System (Pharmacia LKB) and isocratically eluted in 10 mM HEPES, pH 7.5, 1 mM DTT, and 0.15 M NaCl at the same concentration of GuHCl used in the equilibration. All experiments were carried out at 25 °C at a flow rate of 40 μL/min. The column was calibrated in 10 mM HEPES, pH 7.5, 1 mM DTT, and 0.15 M NaCl in the absence of GuHCl with the following proteins of known molecular mass: β-amylase (200 000 Da), cAspATp (92 000 Da), bovine hemoglobin (67 000 Da), and cytochrome *c* (12 300 Da).

Fluorescence measurements were carried out on a Perkin-Elmer LB50S fluorometer, and ellipticity data were collected on a Jasco J500 spectropolarimeter. In both cases, 10 mm cells with thermostatically controlled cell holders were used, the solutions were filtered just before use, and data were corrected by subtracting a control from which the enzyme was omitted. In the fluorescence experiments the bandwidths for excitation and emission were set to 10 and 2.5 nm, respectively, and emission spectra were collected between 310 and 480 nm. Measurements of refolding were achieved by diluting a concentrated solution of denatured protein (2.25 mg/mL incubated for 1 h at 25 °C in 6 M GuHCl) to 3.9 μM at different desired concentrations of GuHCl. Fluorescence spectra were then registered after 1 h at 25 °C.

Kinetics of Reactivation. The kinetics of reactivation were determined as already described for wild-type protein (*30*) with slight modifications. Native holoprotein (3.9 μM) was unfolded for 30 min at 25 °C in 5 M GuHCl, 10 mM HEPES, pH 7.5, 1 mM DTT, and 0.15 M NaCl. Refolding was initiated by rapidly diluting the unfolded protein into the reactivation buffer (10 mM HEPES, pH 7.5, 1 mM DTT, 0.1 mM PMP), preincubated at 0 °C, to a final protein concentration of 78 nM and a final GuHCl concentration of 0.1 M. Samples (40 μL) were removed at intervals and assayed at 5 °C for enzymatic activity in the conventional malate dehydrogenase-linked assay. The progress curve was linear for at least 30 s, and this part of the curve was used to calculate the enzymatic activity.

Constants governing refolding were calculated by nonlinear fitting of experimentally observed activity as a function of refolding time, $A(t)$, to the equation:

$$A(t) = A_\infty + A \exp(-t/\tau) \qquad (5)$$

where A is the amplitude of the kinetic phase, A_∞ is a constant, and τ is the reciprocal of the measured rate constant k.

Computer Data Fitting. Micromath Scientist for Windows was used to analyze the data.

RESULTS

X-ray Crystallographic Analysis. *(A) Space Group Ambiguity*. The first structure of *Ec*AspAT (*18*), as well as all subsequent structures from this and other groups, has been solved in the space group $C222_1$ with one monomer per asymmetric unit (*15*, *31*). In this case the subunits of the functional *Ec*AspAT dimer are related by exact crystallographic symmetry. Jäger and co-workers (*11*) claimed, however, that the true space group of their crystals, although grown under crystallization conditions similar to PEG and ammonium sulfate, is $P2_1$, with pseudo *mmm* symmetry that breaks down at higher resolution. In their crystals the direction of the molecular dyad slightly deviated from that of the crystallographic 2-fold axis in the orthorhombic space group. Thus the asymmetric unit of the crystal contained a dimer rather than a monomer. Slight variations in crystal packing differentiating the two space groups might have been caused by differences in the respective purification or crystallization procedures or by asymmetric binding of the ligand upon soaking. Consequently, a number of *Ec*AspAT structures from this laboratory have appeared in the Protein Data Bank in the monoclinic unit cell. Recently, *Ec*AspAT structures in the open and the closed forms have been published at 1.8 Å resolution in space group $C222_1$, indicating that *mmm* symmetry persists to high resolution (the diffraction data were merged with R_{sym} = 0.041 and 0.045, respectively; see ref *19*). Verification of the *Ec*AspAT coordinate entries with the program WHATIF (*32*) revealed that in all monoclinic *Ec*AspAT entries the subunits can be related by the crystallographic symmetry, and the unit cell can be reduced to the orthorhombic one. To resolve the ambiguity for the present crystals, we processed the diffraction data for the P195A mutant and refined the corresponding structure in both the monoclinic and the orthorhombic unit cells independently. Processing in space group $C222_1$ did not result in any increase in R_{sym} relative to the $P2_1$ case. Also, unlike in ref *11*, no significant differences between the two independent subunits in the asymmetric unit of the $P2_1$ crystal nor deviations of the molecular dyad in the monoclinic cell from the crystallographic dyad in the orthorhombic cell could be established. This indicates that indexing and refinement of these crystals in space group $C222_1$ is feasible. Crystallographic refinement in the lower symmetry space group, although more time-consuming,
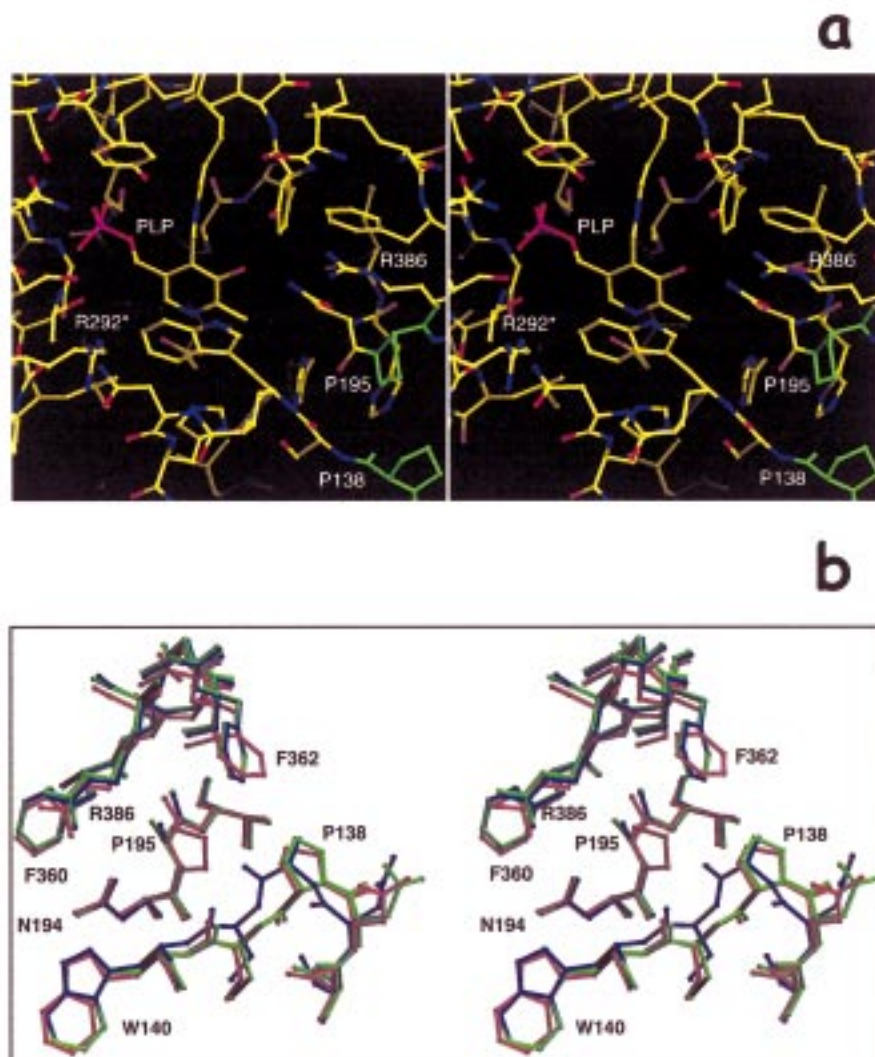
FIGURE 1: Stereoview of the *Ec*AspAT structure in the vicinity of Pro138 and Pro195. (a) View of the site of wild-type *Ec*AspAT through the active site entrance. The amino-terminal helix (residues 10−25) was omitted for clarity. Dicarboxylate substrate binds in front of the PLP ring between Arg292* (asterisk denotes residues from the adjacent subunit) and Arg386, which changes their conformation upon binding (*11*, *33*). Residues Pro138 and Pro195 (green) do not interact with substrate directly but define the positions of the substrate-binding residues Trp140, Asn194, and Arg386. (b) Structural superposition of the wild-type (red), P195A (green), and P195A/P138A (blue) *Ec*AspAT.

would, however, not be erroneous, since any possible asymmetry in the *Ec*AspAT dimer would be accounted for, and the observations-to-parameters ratio is the same in both treatments. Data collection and refinement statistics for the single (P195A) and the double mutant (P138A/P195A) and its complex with the substrate analogue maleate are reported in Table 1.

(B) Structural Consequences of the Mutations. Both Pro138 and Pro195 are located on the surface of the protein close to the active site entrance (Figure 1a). In the wild-type *Ec*AspAT structure Pro138 and Pro195 both occupy *i* + 2 positions in type VIb β-turns (*24*). Substitution of Pro195 with alanine causes only minor changes in the polypeptide chain. The peptide bond preceding Ala195 remains in cis conformation (Figure 1b). The C_β atom of Ala195, however, shifts toward the side chain of the substrate-binding residue Arg386, and it is in direct van der Waals contact with its C_δ atom. The phenyl ring of Phe362, also in a van der Waals contact with the mutated residue, rotates by about 45° to fill the space created by exchanging the pyrolidine ring of Pro195

with a methyl group.

The P138A mutation results in flipping of the Asn137−Ala138 peptide bond to the trans conformation. The ensuing conformational changes involve only residues of the corresponding β-turn, which now belongs to type IV (Figure 1b).

Functional Comparison of Wild-Type EcAspAT and the Mutants. (A) Kinetic and Spectroscopic Characterization. The steady-state kinetics of wild-type and mutant *Ec*AspATs were analyzed with the L-aspartate/2-oxoglutarate substrate pair. All of the mutations yielded active enzymes. However, each mutation produces some change in the catalytic parameters. Both P138A and P195A mutants show a 1.3-fold increase in the k_{cat} value (184 ± 2.9 and 185 ± 6 s^{-1}, respectively) relative to WT (141 ± 2 s^{-1}). All of the mutant enzymes show rather increased K_M values for both 2-oxoglutarate (0.028 ± 0.0016, 0.131 ± 0.0045, 0.45 ± 0.0025, and 0.13 ± 0.011 mM for WT, P138A, P195A, and P138A/P195A, respectively) and aspartate (0.46 ± 0.02, 1.61 ± 0.06, 4.64 ± 0.25, and 3.58 ± 0.26 mM for WT, P138A, P195A, and P138A/P195A, respectively). It can be observed that

Table 2: Limiting Rate Constant for Cyanoborohydride Reduction at Saturating Maleate Concentrations[a]

enzyme	k'/r (M^{-1} s^{-1})
WT	0.078 ± 0.003
P138A	0.11 ± 0.009
P195A	0.47 ± 0.08
P138A/P195A	0.23 ± 0.03

[a] The limiting rate constant k'/r was calculated from the k' and r values determined by fitting the experimental rate of cyanoborohydride reduction at different maleate concentrations to eq 3, as described under Materials and Methods.

P195A is the mutation that affected the affinity for substrates mostly.

No substantial change can be observed in the spectroscopic characteristics of the aspartate aminotransferase's coenzyme, pyridoxal 5′-phosphate (PLP) [pK_a values in the absence and in the presence of saturating concentrations of maleate, a dicarboxylate substrate analogue, which is known to increase the pK_a of the internal imine and to induce the open to closed conformational change of the enzyme (*33, 34*)].

(B) Ligand-Induced Conformational Change. The reducibility of the aldimine formed between PLP and Lys258 by sodium cyanoborohydride proved to be a useful tool in determining the open/closed conformational status of aspartate aminotransferase (*29*). Rates of reduction were determined in the presence of increasing concentrations of maleate for all of the mutants in comparison with wild-type enzyme. The reaction was monitored by measuring the increase at 340 nm due to reduction of the aldimine double bond. Reactions were apparently first order at all ligand concentrations, and the apparent rate constant decreased hyperbolically with increasing ligand concentration. As already described in the case of porcine cytosolic aspartate aminotransferase (*29*) and observed for the *E. coli* wild-type aspartate aminotransferase (A. Garnier, personal communication), the fall in rate of borohydride reduction reaches a limiting value at saturating dicarboxylate concentrations. This value, as shown in Table 2, varies depending on the mutation. Since the finite reducibility at saturating concentrations of maleate can be related to the fraction of the enzyme in the open conformation (*29*), it can be suggested that in the case of the P195A mutant the equilibrium is more shifted toward the open conformation in comparison with wild type.

Thermal Denaturation. Thermal unfolding transitions were measured for wild-type protein and the *cis*-proline mutants. The progress of unfolding was monitored by following the amide ellipticity at 221 nm as a probe for changes in secondary structure upon increasing temperature. The thermal unfolding curves, normalized by fitting baselines below and above the transition zone, are shown in Figure 2. The midpoint of the thermal transition is at 67 °C for wild type, in a fairly good agreement with the reported melting temperature of 65.5 °C determined by differential scanning calorimetry (*35*), at 66 °C for P138A, and at 63 °C for P195A and P138A/P195A. Differential scanning calorimetry experiments of WT showed two endotherms and an incomplete reversibility of the thermal denaturation, thus demonstrating that a two-state thermal unfolding model is not applicable to these proteins (*35*). Therefore, since a full thermodynamic characterization of these proteins is not possible, only T_m (midpoint of thermal transition) values can be taken into
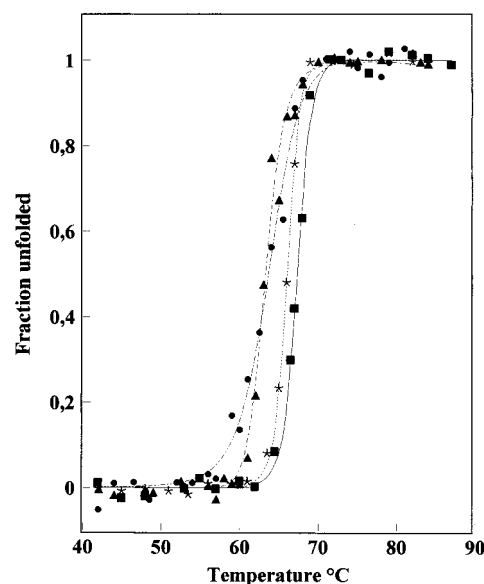

FIGURE 2: Thermal transition curves for wild-type (■), P138A (∗), P195A (▲), and P138A/P195A (●) as monitored by CD spectroscopy. The enzyme concentration was 3.9 μM in 10 mM HEPES, 1 mM DTT, and 0.15 M NaCl, pH 7.5. The fraction unfolded was calculated from the observed ellipticity at 222 nm using eq 4. Lines through data were drawn to aid the eye.

consideration. Nevertheless, the data suggest that the substitutions have very small effects on the thermal stability of the proteins, the T_m being shifted only one to four degrees relative to wild-type protein, depending on the mutation.

GuHCl-Induced Unfolding Transition. GuHCl-induced unfolding of *Ec*AspAT at 20 °C is reversible and has been shown to proceed through the formation of at least two monomeric intermediates, along the unfolding pathway (*36*):

$$N_2 \rightleftharpoons 2M \rightleftharpoons 2M^* \rightleftharpoons 2U$$
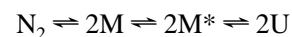
where N_2 is the native dimer, M and M* are distinct "structured" monomers, and U is the unfolded state. The effects of the mutations in the unfolding pathway, in the relative stability, and/or in the structure of the intermediates have been investigated using gel filtration, tryptophan fluorescence, and far-ultraviolet circular dichroism.

All of the mutants are inactivated upon 1 h incubation at 25 °C in 6 M GuHCl in 10 mM Na-HEPES, 1 mM DTT, and 0.15 M NaCl. The proteins recover between 90% and 100% of the original activity within 1 h when the denatured enzyme is 60-fold diluted at 0 °C in 0.1 M Na-HEPES, 1 mM DTT, 0.15 M NaCl, 0.1 mM PMP, and 2 mM 2-oxoglutarate.

No evident difference was detected in the gel filtration experiments in GuHCl at equilibrium carried out with the different mutants as with the holoenzyme of WT protein (*37*) (data not shown), leading to the conclusion that, as far as can be detected in a gel filtration analysis, the dissociation event in the unfolding pathway is almost unaffected by the mutations.

The unfolding process is clearly biphasic for all of the mutants, and a stable intermediate state identified as the M* reported by Herold and Kirschner for WT (*36*) can be observed in all cases by following the bathochromic shift of the fluorescence maximum and the decrease of the CD signal
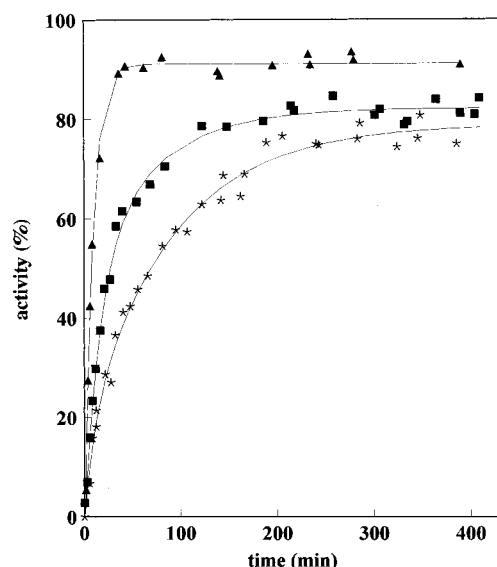
FIGURE 3: Reactivation kinetics of denatured WT (■), P138A (∗), and P195A (▲). Native proteins (3.9 µM) were unfolded for 30 min at 25 °C in 5 M GuHCl, 10 mM HEPES, pH 7.5, 1 mM DTT, and 0.15 M NaCl. Reactivation was started by rapidly 50-fold diluting the unfolded protein into the reactivation buffer (10 mM HEPES, pH 7.5, 1 mM DTT, 0.1 mM PMP) preincubated at 0 °C. Reactivation was followed as described under Materials and Methods. Continuous lines are those of best fit to data using eq 5.

at 221 nm as the concentration of GuHCl is increased (data not shown).

The emission maxima of the native fluorescence spectra of P195A and P138A/P195A are blue shifted by 2 and 2.5 nm, respectively, relative to WT. The emission maxima of the fluorescence spectra of the intermediate state M* of P195A is red shifted by 2 nm, while P138A and P138A/P195A are both red shifted by 5.5 nm relative to WT. These shifts are significant since variations in several spectra never exceeded ±0.5 nm.

The data are indicative of a slightly more compact intermediate for the P138A, with the tryptophan residues responsible for the fluorescence of the M* intermediate less exposed in P138A than in WT and P195A, as also confirmed in iodide quenching experiments carried out on the M* (data not shown).

Kinetics of Reactivation. The progress curves of reactivation at 0 °C of WT, P138A, and P195A after 30 min of unfolding in 5 M GuHCl are shown in Figure 3. In all cases, the progress curves begin at the origin, showing no rapid phase of reactivation. The progress curves can be described as a single exponential. Attempts to fit them to a double exponential, as reported by Leistler and colleagues (*30*) for wild-type protein, failed. As already stated, all of the proteins regain between 80% and 100% of the initial activity. A time constant *t* of 28 min was calculated for the renaturation curve of wild-type, 83 min for P138A, and 9 min for P195A.

DISCUSSION

The *cis*-prolines at positions 138 and 195 of aspartate aminotransferase are among the very few residues (11 out of about 400 in the polypeptide chain) that are conserved throughout evolution, from bacteria to mammals to archaea. Surprisingly, we have found that *cis*-prolines 138 and 195 are not essential for the protein architecture and functional

structure of aspartate aminotransferase from *E. coli*: mutants at the two *cis*-prolines of *Ec*AspAT retain the homodimeric quaternary structure and, although less efficient than wild type, retain a high catalytic activity. Moreover, all the changes observed, in the structure and in the catalytic properties, are surprisingly small.

In the wild-type *Ec*AspAT structure Pro138 and Pro195 are in direct van der Waals contact with each other. Together with Pro16, Pro141, Phe362, and Val382 they form a nonpolar ring near the mouth of the active site entrance. Although these *cis*-prolines in *Ec*AspAT do not make direct contacts with substrate, they are both in β-turns responsible for correct positioning of the critical substrate-binding residues Trp140 and Asn194 (Figure 1a). The two β-turns also flank a cluster of conserved residues, His143, His189, and His193, near the coenzyme-binding site.

Upon substitution of *cis*-Pro195 with *cis*-Ala195, only minor changes in the polypeptide chain were observed. The new orientation of the phenyl ring of Phe362, which was observed in both the single and the double mutant, increases the "friction" between the small and the large domains upon domain closure through direct interaction with Ser384. These two newly created contacts between the domains might account for the shift in equilibrium toward the open conformation observed in the sodium cyanoborohydride reduction reaction and for the slight increase in K_M value of all substrates. Spectroscopic results, combined with the sodium cyanoborohydride reduction kinetics, seem to be indicative of an effect of the P195A mutation on the domain opening−closing dynamics rather than on the chemistry of the active site.

It can be argued that a cis conformation might play a relevant role at position 195, since even an alanine in this position adopts this otherwise very rare conformation. In wild-type *Ec*AspAT the main chain carbonyl oxygen of Asn194 is located between the imidazole rings of His189 and His193. A switch to the trans isomer would bring it in direct contact with Phe360 and would disrupt favorable interactions made by the side chains of His193 and Asn194. Structural constraints, therefore, force the peptide bond at position 195 to adopt the cis conformation despite the substitution.

The cis conformation at position 138, instead, is not essential for the protein, since the P138A mutation results in flipping of the Asn137−Ala138 peptide bond to the trans conformation. The conformational rearrangement of the corresponding β-turn seems to have less impact on the catalytic properties of the enzyme, probably because it is more remote from the domain interface. In the trans conformation the carbonyl group of Asn137 forms a new hydrogen bond with a hydroxyl group of Ser136. Due to the fewer contacts made by the loop containing position 138, the conformational changes associated with cis−trans isomerization can be easily accommodated by the rest of the structure, and a switch to the trans conformation does occur.

The replacement of the *cis*-prolines does not perturb the stability of *Ec*AspAT to any significant extent. Often, the replacement of a *cis*-proline residue has been reported to destabilize protein structure, whether the substituted amino acid forms a cis peptide bond or not (see below). If a trans bond replaces the cis bond, the geometry of the main chain in the folded conformation has to accommodate the distortion

thus generated; if the cis conformation is retained, the course of the main chain is preserved, but the free energy of the folded protein increases. Moreover, quite apart of the secondary effects introduced by the mutations, Pro to Ala substitutions are expected to destabilize the protein due to the increase in the entropy of unfolding they induce. This has usually indeed been found experimentally. For example, the replacement of any of the two *cis*-proline residues of pancreatic RNase A was reported to decrease its thermal stability by about 10 kJ/mol (*38*). Even more dramatic is the case of *E. coli* thioredoxin, where mutation of the only *cis*-proline shifted the melting temperature downward from 82 °C to 65 °C (*39*). In RNase T1 the substitution of the cis Ser54−Pro55 peptide bond by a trans Gly54−Asn55 did not change the structure and stability to a significant extent (*7*). The retention, however, of the cis peptide bond in the *cis*-Pro39 to Ala mutant of RNase T1 is accompanied by a strongly destabilizing effect of about 20 kJ/mol (*40, 41*). In the *cis*-Pro202 to Ala mutant of carbonic anhydrase II, the only other reported case where the cis peptide bond has been proved to be retained despite the mutation, the substitution of *cis*-alanine for *cis*-proline decreased the stability of the folded state by about 5 kcal/mol relative to both the unfolded state and an equilibrium unfolding intermediate in guanidine hydrochloride-induced denaturation (*42*). In the case of *Ec*AspAT, only the mutation at position 195 can be considered slightly destabilizing. Its effect is not dramatic, however, since the melting temperature is shifted down by only 4°. It can be argued that Pro138 is located in a loop on the surface of the protein, and the change in main chain geometry due to the peptide flip can be easily accommodated. The P195A mutation in *Ec*AspAT is the first example of a cis conformation being retained in a *cis*-Pro mutant without a substantial destabilizing effect. The reason for this could lie in part in the fact that AspAT is a much larger protein than the usual model proteins, such as RNases and carbonic anhydrases, and therefore, the protein architecture can probably more easily dissipate an unfavorable mutation. The stability of these mutants will have another favorable "indirect" effect in the analysis of refolding kinetics, since frequently slower folding kinetics reflect only a strong destabilization of the folded state caused by mutations (*43*).

The reactivation processes of the *cis*-proline mutants of *Ec*AspAT also provided surprising results. The P195A mutant, indeed, where a *cis*-Ala substituted a *cis*-Pro, showed a recovery of enzymatic activity after GuHCl-induced unfolding faster than wild type, whereas the reactivation of P138A, in which a *cis*-Pro has been replaced by a *trans*-Ala, was slower, even slower than wild type. This behavior is quite unusual: a reactivation slower than wild type would have been expected from a mutant with a *cis*-nonprolyl peptide bond, whereas a reactivation faster or as fast as wild type would have been expected from a protein with one cis peptide bond less than wild type. Therefore, a direct connection between cis−trans isomerization at positions 138 and 195 and folding of *Ec*AspAT cannot be easily depicted. Other types of conformational rearrangement reactions appear to govern the folding process of this protein under strongly folding conditions. However, cis−trans isomerization at positions 138 and 195 still seems to play some role, since the reactivation behavior is sensibly changed by the mutations, and the differences observed have to be ascribed to the effects created by the replacement of the proline with alanine. The three-dimensional structures of the mutants, indeed, are nearly the same as that of wild type except for the immediate surroundings of the mutated positions. Structure formation and proline isomerization are mutually interdependent during refolding: tertiary structure interactions may favor proline isomerization and vice versa, in a cooperative view of the protein-folding process. It has been documented (*44*) that the presence of structured intermediates can lead to a marked increase of proline isomerization while a hindrance of prolyl isomerization by premature structure formation was observed in the refolding of RNase T1 (*45*). In the case of *Ec*AspAT, we suggest that the likely destabilization of a folding intermediate with a cis peptide bond at position 195, caused by the substitution of Pro with Ala, leads to a strong acceleration of the overall reactivation reaction, whereas specific favorable tertiary interactions in some folding intermediates are favored by cis−trans isomerization at position 138.

In conclusion, *cis*-prolines seem to have been retained throughout the evolution of aspartate aminotransferase to possibly play a subtle role in directing the traffic of intermediates toward the unique structure of the native state, rather than to respond to the needs for a specific structural role.

REFERENCES

1. Nall, T. (1994) in *Mechanism of Protein Folding* (Pain, R. H., Ed.) pp 80−103, Oxford University Press, Oxford, England.
2. Schmid, F. X. (1992) in *Protein Folding* (Creighton, T. E., Ed.) pp 197−241, Freeman, New York.
3. Šali, A., and Overington, J. P. (1994) *Protein Sci. 3*, 1582−1596.
4. Matthews, B. W., Nicholson, H., and Becktel, W. J. (1987) *Proc. Natl. Acad. Sci. U.S.A. 84*, 6663−6667.
5. Kelley, R. F., and Richards, F. M. (1987) *Biochemistry 26*, 6765−6774.
6. Schultz, D. A., Schmid, F. X., and Baldwin, R. L. (1992) *Protein Sci. 1*, 917−924.
7. Kiefhaber, T., Grunert, H. P., Hahn, U., and Schmid, F. X. (1990) *Biochemistry 29*, 6475−6480.
8. Mehta, P. K., Hale, T. I., and Christen, P. (1993) *Eur. J. Biochem. 214*, 549−561.
9. John, R. A. (1996) *Biochim. Biophys. Acta 1248*, 81−96.
10. Mehta, P. K., Hale, T. I., and Christen, P. (1989) *Eur. J. Biochem. 186*, 249−253.
11. Jäger, J., Moser, M., Sauder, U., and Jansonius, J. N. (1994) *J. Mol. Biol. 239*, 285−305.
12. Ovchinnikov, Y. A., Egorov, C. A., Aldanova, N. A., Feigina, M. Y., Lipkin, V. M., Abdulaev, N. G., Grishin, E. V., Kiselev, A. P., Modyanov, N. N., Braunstein, A. E., Polyanovsky, O. L., and Nosikov, V. V. (1973) *FEBS Lett. 29*, 31−34.
13. McPhalen, C. A., Vincent, M. G., Picot, D., Jansonius, J. N., Lesk, A. M., and Chothia, C. (1992) *J. Mol. Biol. 227,* 197−213.

14. Yano, T., Kuramitsu, S., Tanase, S., Morino, Y., Hiromi, K., and Kagamiyama, H. (1991) *J. Biochem. (Tokyo),* 813−816.

15. Kamitori, S., Hirotsu, K., Higuchi, T., Kondo, K., Inoue, K., Kuramitsu, S., Kagamiyama, H., Higuchi, Y., Yasuoka, N., Kusunoki, M., and Matsuura, Y. (1987) *J. Biochem. (Tokyo) 101*, 813−816.

16. Birolo, L., Sandmeier, E., Christen, P., and John, R. A. (1995) *Eur. J. Biochem. 232*, 859−864.

17. Kuramitsu, S., Hiromi, K., Hayashi, H., Morino, Y., and Kagamiyama, H. (1990) *Biochemistry 29*, 5469−5476.

18. Smith, D. L., Almo, S. C., Toney, M. D., and Ringe, D. (1989) *J. Mol. Biol. 209*, 499−501.

19. Okamoto, A., Higuchi, T., Hirotsu, K., Kuramitsu, S., and Kagamiyama, H. (1994) *J. Biochem. (Tokyo) 116*, 95−107.

20. Kabsch, W. (1988) *J. Appl. Crystallogr. 21*, 916−924.

21. Navaza, J. (1994) *Acta Crystallogr., Sect. A 50*, 157−163.

22. Jones, T. A., Zou, J.-Y., Cowan, S. W., and Kjelgaard, M. (1991) *Acta Crystallogr. D47*, 110−119.

23. Tronrud, D. E., Ten Eyck, L. F., and Matthews, B. W. (1987) *Acta Crystallogr. A43*, 489−501.

24. Hutchinson, E. G., and Thornton, J. M. (1996) *Protein Sci. 5*, 212−220.

25. Karmen, A. (1955) *J. Clin. Invest. 34*, 131−133.

26. Velick, S. F., and Vavra, J. (1962) *J. Biol. Chem. 237*, 2109−2122.

27. Fasella, P., Giartosio, A., and Hammes, G. G. (1966) *Biochemistry 5*, 197−202.

28. Goldberg, J., Swanson, R. V., Goodman, H. S., and Kirsch, J. F. (1991) *Biochemistry 30,* 305−312.

29. Garnier, A., and John, R. A (1993) *Eur. J. Biochem. 216*, 763−768.

30. Leistler, B., Herold, M., and Kirschner, K. (1992) *Eur. J. Biochem. 205*, 603−611.

31. Kamitori, S., Hirotsu, K., Higuchi, T., Kondo, K., Inoue, K., Kuramitsu, S., Kagamiyama, H., Higuchi, Y., Yasuoka, N., Kusunoki, M., and Matsuura, Y. (1988) *J. Biochem. (Tokyo) 104*, 317−318.

32. Vriend, G. (1990) *J. Mol. Graphics 8*, 52−56.

33. Jansonius, J. N., and Vincent, M. G. (1987) in *Biological Macromolecules and Assemblies* (Jurnak, F. A., and McPherson, A., Eds.) Vol. 3, pp 187−285, John Wiley and Sons, New York.

34. Picot, D., Sandmeier, E., Thaller, C., Vincent, M. G., Christen, P., and Jansonius, J. N. (1991) *Eur. J. Biochem. 196*, 329−341.

35. Gloss, L. M., Planas, A., and Kirsch, J. F. (1992) *Biochemistry 31*, 32−39.

36. Herold, M., and Kirshner, K. (1990) *Biochemistry 29*, 1907−1913.

37. Herold, M., and Leistler, B. (1992) *FEBS Lett. 308*, 26−29.

38. Schultz, D. A., and Baldwin, R. L. (1992) *Protein Sci. 1*, 910−916.

39. Kelley, R. F., and Richards, F. M. (1987) *Biochemistry 26*, 6765−6774.

40. Mayr, L. M., Landt, O., Hahn, U., and Schmid, F. X. (1993) *J. Mol. Biol. 231*, 897−912.

41. Mayr, L. M., Willbold, D., Rösch, P., and Schmid, F. X. (1994) *J. Mol. Biol. 240*, 288−293.

42. Tweedy, N. B., Nair, S. K., Paterno, S. A., Fierke, C. A., and Christianson, D. W. (1993) *Biochemistry 32*, 10944−10949.

43. Jennings, P. A., Saalau-Bethell, S. M., Finn, B. E., Chen, X., and Matthews, C. R. (1991) *Methods Enzymol. 202*, 113−126.

44. Schmid, F. X. (1986) *FEBS Lett. 198*, 217−220.

45. Kiefhaber, T., Grunert, H. P., Hahn, U., and Schmid, F. X. (1992) *Proteins: Struct., Funct., Genet. 12*, 171−179.